Research in Astron. Astrophys. **2010** Vol. **10** No. **6**, 541–552
http://www.raa-journal.org *http://www.iop.org/journals/raa*

***R**esearch in*
***A**stronomy and*
***A**strophysics*

Rotation curve of the Galactic outer disk derived from radial velocities and UCAC3 proper motions of carbon stars *

Jia-Cheng Liu[1,2] and Zi Zhu[1,2]

[1] Department of Astronomy, Nanjing University, Nanjing 210093, China; *jcliu@nju.edu.cn*
[2] Key Laboratory of Modern Astronomy and Astrophysics (Nanjing University), Ministry of Education, Nanjing 210093, China

Received 2010 January 4; accepted 2010 March 10

Abstract The availability of astrometric data and radial velocities of carbon stars near the Galactic plane enables us to investigate the kinematics of the Milky Way, especially the rotation curve. The recently published Third U. S. Naval Observatory CCD Astrograph Catalog (UCAC3) provides the opportunity to test this problem using three-dimensional velocity in order to obtain more reliable rotation curves. We intend to study the Galactic rotation curve up to $15\,\mathrm{kpc}$ using the radial velocities and proper motions of carbon stars. The motivation for using UCAC3 is to provide high precision proper motions which have hardly been used in determining the rotation velocity of tracers. Seventy-four carbon stars and carbon-rich Mira variables toward the anti-center direction $(90^\circ < \ell < 270^\circ, |b| < 6^\circ)$ are picked up from the literature then matched with UCAC3 carbon star candidates to obtain their proper motions. A rigorous geometrical method is employed to compute the rotation velocity of each object. Taking carbon stars as tracers, we find a flat rotation curve of $210 \pm 12\,\mathrm{km\,s^{-1}}$ assuming $R_0 = 8.0\,\mathrm{kpc}$ for the galactocentric distance and $V_0 = 220\,\mathrm{km\,s^{-1}}$ for the rotation velocity of the Sun. Due to the uncertainties of distances, the rotation velocities are more dispersed if tangential velocities enter the calculation, compared to those derived from radial velocities only. However, the whole rotation curve shows coherence with previous results. Increasing observation and study of carbon stars would be desirable in order to provide more homogeneous data for the kinematical study of the Galactic disk.

Key words: astrometry — Galaxy: disk — Galaxy: kinematics and dynamics — stars: carbon

1 INTRODUCTION

The profile of the rotation curve of the Milky Way is very important, because of its crucial role in determining the distribution of dark matter in the Galaxy. Following the confirmation of the galactocentric distance of the local standard of rest (LSR) and its rotation velocity, the characteristics of kinematical properties, including the rotation curve, can be explored by observing the distance and relative motion of the stars with respect to the Sun. Rotation curves of spiral galaxies have been

* Supported by the National Natural Science Foundation of China.

investigated by many authors via different methods. It is now generally understood that the rotation curves of spiral galaxies, including our Milky Way, are neither rigid $V(R) \propto R$ nor Keplerian $V(R) \propto R^{1/2}$. The curve of the inner disk can be determined by an ingenious tangent-point method using HI gas (Blitz & Spergel 1991) while the rotation curve for $R > R_0$ has proved hard to measure, because of the solar location in the middle of the Galactic plane. The rotation curve of the outer disk has been studied using HII regions (Fich et al. 1989). According to the classical cepheids method proposed by Pont et al. (1994, 1997), the rotation curve is flat and slightly decreasing between R_0 and $2R_0$, which has a mismatch of $30\,\mathrm{km\,s^{-1}}$ compared to the HII region curve.

Similar to classical cepheids, carbon (C) stars, first identified in the Milky Way in the 1960s (Westerlund 1965), are popular for studying the kinematics of the Galactic disk because they are considered as reliable standard candles (Battinelli & Demers 2005) for stars and external galaxies. Known as luminous asymptotic giant branch (AGB) giants, C stars can be confirmed spectroscopically on the $(J-K)$ vs. K color-magnitude diagram (CMD). The absolute magnitude M_K shows a small dispersion for N-type C stars under certain color and magnitude restrictions (Weinberg & Nikolaev 2001). More recently, Demers & Battinelli (2007) in their study clearly show a rotation curve of the outer disk from 9 to $15\,\mathrm{kpc}$ using radial velocities of 35 carbon stars for galactic longitude $60^\circ < \ell < 150^\circ$ (their fig. 4). In fact, in these processes of studying rotation of the outer disk, independently determined radial velocities and distances of a population of tracers were used with the circular-motion assumption, while the transverse velocities were neglected. This motivates us to re-examine this problem by putting proper motions in the computation.

Thanks to the data released from the UCAC3 catalog (Zacharias et al. 2010) in October 2009, the precise astrometric parameters of C stars could easily be obtained, which gave us confidence to do a comprehensive study on the rotation property of the Galactic disk. In Section 2, we firstly present a snapshot of the data that we shall use. Section 3 presents our methods and resulting rotation curves. The discussion and conclusions are given in Sections 4 and 5.

2 DATA OF CARBON STARS NEAR THE GALACTIC PLANE

2.1 Raw Data

The goal in data selection is to find C stars near the Galactic plane with complete velocity components. From the literature, carbon stars and carbon-rich Miras variables are admitted. These involve the following three parts:

- The list of cool carbon stars near the Galactic plane is compiled by Demers & Battinelli (2007), which contains 103 C star candidates in the area ($60^\circ < \ell < 220^\circ, 3^\circ < |b| < 5^\circ$) and 75 entries identified as C stars from the spectral observation in October, 2006. The distances and radial velocities are provided in the sample. Because our restriction of sky area, as mentioned before, is $90^\circ < \ell < 270^\circ$, 65 sources enter our C star list.
- Millimeter observed infrared carbon stars are from IRAS (Groenewegen et al. 2002). 330 all-sky distributed infrared C stars are presented in their table 1. Toward the anti-center direction area near the disk, 85 carbon stars were picked up with heliocentric distances up to about $5.5\,\mathrm{kpc}$.
- Catalog of 177 C-Miras with estimated distances and radial velocities is from Menzies et al. (2006) in which there are 44 entries in the our area of interest. The distances are based on the bolometric magnitudes observed by the South African Astronomical Observatory (SAAO) and true radial velocities of the variables are derived from a comparison between optical and CO mm observations.

Figure 1 displays the distribution of 194 selected carbon stars in the Galactic plane. Carrying out cross identification, we find that 16 of them appear in two of the three source catalogs while none of the carbon stars appear in all of the three source C star lists. In the case of overlap, the mean values of heliocentric distances and radial velocities of the common objects are adopted as the final value.

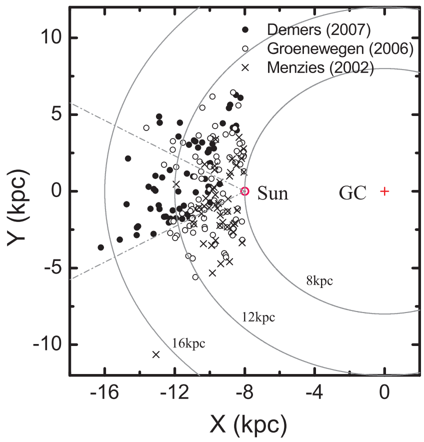

Fig. 1 Positions of 194 carbon stars on the Galactic plane. X and Y are coordinates in kpc, pointing to the Galactic center and to the direction of Galactic rotation, respectively. The Galactic center is at the origin, thus the Sun is at the coordinates ($-R_0$, 0). Filled circles refer to carbon stars from Demers & Battinelli (2007); open circles from Groenewegen et al. (2002) and crossing lines from Menzies et al. (2006). Circles are indicated at $R = R_0$, $R = 12\,\mathrm{kpc}$, and $R = 16\,\mathrm{kpc}$. The dash-dotted lines denote the direction $\ell = 150°$ and $\ell = 210°$ (see Sect. 3).

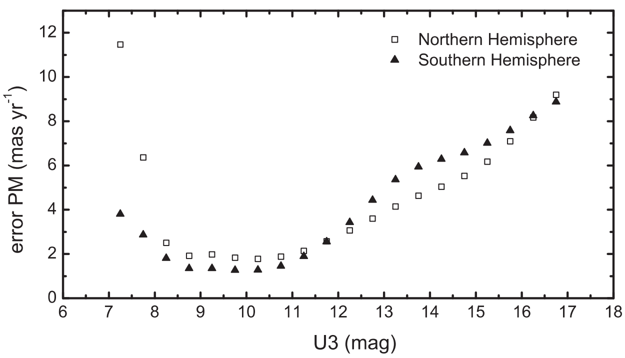

Fig. 2 Mean, formal errors of UCAC3 proper motions as a function of UCAC3 bandpass magnitudes. The open squares and filled triangles are for the northern and southern hemispheres, respectively.

UCAC3 is used here as the resource of proper motions to obtain the transverse velocities of C stars. It is the latest release of the ongoing UCAC project, designed to observe the entire sky covering mainly the 8 to 16 magnitude range in a single bandpass between V and R. It is also a high density, precise astrometric catalog of more than 100 million stars. The position errors are about 15 to $20\,\mathrm{mas}$ for stars brighter than $14\,\mathrm{mag}$, and the errors in proper motions relative to the UCAC3 magnitude are shown in Figure 2. The C stars with high absolute luminosity ($M_R \approx -3.5\,\mathrm{mag}$) have UCAC3 magnitude between 11–13 mag, thus the error range of proper motions of the C stars is $3 - 6\,\mathrm{mas\,yr^{-1}}$. According to the analysis of UCAC2 (Zacharias et al. 2004), the external systematics of proper motion of the improved UCAC3 should be better than $1.0\,\mathrm{mas\,yr^{-1}}$. The UCAC3 is an appropriate catalog in the present study of C stars and Galactic kinematics for the following reasons: 1) UCAC3 is a high density catalog of deep observation; 2) the astrometric precision is unprecedentedly high compared to other catalogs that contain stars of the same order; 3) the Two Micron All-Sky Survey (2MASS) near-infrared magnitudes JHK are provided based on which C stars can be easily identified.

The General Catalog of Galactic Carbons Stars, 3rd edition, hereafter CGCS3 (Alksins et al. 2001), consists of 6891 individual positions, magnitudes, and spectral types for C stars. It is used to match the positions directly to the selected C star candidates for the purpose of further investigation (see Sect. 4). The positions of the sources are found to be accurate to within roughly 2 arcsec at the epoch of J2000.0.

2.2 UCAC3 Carbon Star List

Considerable efforts have been made in order to find C stars, both in and out of the Galaxy. Spectroscopically confirmed C stars were found at the red end of the $J-K$ vs. K plane. Nikolaev & Weinberg (2000), in their study of LMC 2MASS data, set the blue limit of the C star at $(J-K)_0 = 1.4$. Other authors (Kang et al. 2006; Cioni & Habing 2003; Davidge 2005) have also come to similar conclusions, leading to $(J-K)_0 > 1.4$ and $(H-K)_0 > 0.45$ as the principal characteristic of C stars. We applied these color limits to the normal exposed single stars (in the UCAC3 catalog, type flag objt=0 or objt=1, and double star flag dsf=0) in the anti-center area and found 84 131 objects. We called this the "UCAC3 C star candidate list." However, no absorption or reddening calibration was applied during the process of selecting stars. Battinelli et al. (2007) pointed out that the present adopted color limit cannot be used to properly separate M and C stars, thus the method does not produce a pure sample.

The C stars (194 in total) from three cited papers (Demers & Battinelli 2007; Groenewegen et al. 2002; Menzies et al. 2006) were searched for, by a main criterion of position coincidence as well as photometric information, in the "UCAC3 C star candidate list." Considering the accuracy of the positions of the stars in the literature, the basic matching criterion is the coordinates of a position agreeing to within $3\,\mathrm{arcsec}$ and a magnitude agreement to within $0.1\,\mathrm{mag}$. If more than one match occurred, the nearest neighbor was chosen. As a result, 50, 14 and 13 stars are recognized separately, with 3 objects in two source catalogs of C stars. Table 1 exhibits the resulting C stars with measurements of positions, heliocentric distance, radial velocities and UCAC3 proper motions. The spacial distribution of the sample is displayed in Figure 3. The lack of objects near scale height $z = 0$ is due to the high reddening in the extremely low latitude. The list contains 74 objects which have K magnitudes between 2.2 and 12.6, 51 in the south and 23 in the north. This reflects the uneven distribution of C stars (Blanco 1965).

3 GALACTIC ROTATION

3.1 Working with Radial Velocities Only

With the distances and radial velocities provided in the literature, the rotation curve based on the sample can be determined.

Assuming a circular rotation around the Galactic center, in other words, the stars are moving in rigorous circular orbits, the rotation velocity of the star at the position (ℓ, b, d) is:

$$V_{\mathrm{rot}} = \left(\frac{V_r + V_{\odot r}}{\sin\ell\cos b} + V_0\right)\frac{R}{R_0}, \tag{1}$$

where V_r is the heliocentric radial velocity and $V_{\odot r} = U_\odot \cos\ell\cos b + V_\odot \sin\ell\cos b + W_\odot \sin b$ is the projection of the solar motion on the line of sight. We adopt the latest values of components of solar motion suggested by Aumer & Binney (2009): $U_\odot = 9.96$, $V_\odot = 5.25$, $W_\odot = 7.07$ and

Table 1 Carbon Star List ($90^\circ < \ell < 270^\circ, |b| < 6^\circ$) Obtained from UCAC3 and Three Cited Papers

ID	Name	$\alpha\,(^\circ)$	$\delta\,(^\circ)$	d (kpc)	μ_ℓ^* (mas yr^{-1})	μ_b (mas yr^{-1})	V_r (km s^{-1})
1	V328 Cas	8.906.	58.007	3.60	–0.532	2.738	–69.0
2	CGCS 111	11.574	59.628	3.30	0.236	–3.205	–36.0
3	W Cas	13.724	58.563	1.46	–7.156	–3.297	–44.3
4	V645 Cas	19.720	58.159	3.40	–0.745	–4.304	–62.0
5		21.329	57.655	4.00	3.088	3.335	–52.0
6		23.567	57.724	3.30	–3.811	–2.061	–72.0
7		25.536	57.926	5.80	–7.179	–5.921	–100.0
8	V918 Cas	25.993	58.685	3.30	–1.064	0.699	–36.0
9	IRAS 01443+6417	26.983	64.549	2.49	–18.297	16.948	–68.1
10	CGCS 282	27.732	57.481	4.30	–1.345	–4.323	–35.0
11	EW Per	28.065	56.967	4.40	5.574	–0.508	–82.0
12	CN Per	31.665	56.852	3.90	0.728	0.010	–38.0
13		35.240	56.389	6.90	2.327	1.798	–64.0
14		37.416	56.192	4.40	–1.132	0.948	–35.0
15	LR Per	38.193	56.491	5.20	–4.133	–0.733	–25.0
16	DY Per	38.821	56.146	2.70	8.484	3.816	–38.0
17	CGCS 381	39.536	56.351	6.60	–0.186	–5.319	–35.0
18	IRAS 04127+5030	64.138	50.626	2.80	3.991	–2.264	0.30
19	CGCS 702	67.505	41.841	2.40	1.413	–4.626	–38.0
20	CGCS 708	67.733	41.571	3.50	–3.322	–2.233	–58.0
21	CGCS 726	69.321	40.783	7.00	–0.724	–4.996	–14.0
22	AU Aur	73.563	49.900	1.53	7.468	3.995	–14.7
23	DS Aur	77.615	33.994	2.10	–17.602	18.661	49.0
24	CGCS 873	77.909	46.285	3.10	–6.950	–3.776	34.0
25	CGCS 975	83.408	40.475	5.20	–3.343	–16.651	–1.0
26	CGCS 985	83.677	40.261	4.80	8.546	35.844	–16.0
27	IRAS 05428+1215	86.414	20.695	1.25	3.165	–2.496	15.0
28		89.161	14.958	5.00	5.384	–3.866	70.0
29		89.193	16.542	5.50	–5.332	–1.788	33.0
30	CGCS 1107	89.202	30.836	5.10	–7.316	11.729	14.0
31	V508 Aur	89.312	32.378	5.20	8.012	–31.236	–12.0
32	CGCS 1130	90.218	30.757	3.80	10.182	0.328	35.0
33	BQ Aur	90.432	29.455	2.10	–1.401	7.684	33.0
34		90.691	29.646	2.80	–0.425	–1.367	40.0
35	IRAS 06032+1157	91.524	11.961	3.90	3.101	–14.854	59.0
36	CGCS 6115	92.715	9.736	4.90	5.101	6.675	51.0
37	CGCS 6117	93.073	9.351	4.80	1.594	23.661	52.0
38	CGCS 6122	93.725	8.666	6.60	25.367	–24.412	64.0
39	CGCS 1214	94.027	6.777	4.60	8.282	1.930	36.0
40	CGCS 6129	94.405	9.627	6.50	64.979	–32.780	96.0
41		95.071	25.076	6.80	2.678	1.868	47.0
42	CGCS 1238	95.166	5.883	4.30	–10.035	1.342	49.0
43	V615 Mon	95.474	6.441	7.80	–2.675	–7.256	66.0
44	IRAS 06192+0722	95.492	7.349	2.86	–12.118	–1.736	15.2
45	V617 Mon	95.949	8.498	2.81	–0.667	2.162	8.9
46	ZZ Gem	96.005	25.031	1.69	1.664	0.602	66.8
47	CGCS 1311	98.693	17.777	3.60	10.214	–14.986	76.0
48	CGCS 6168	103.249	9.277	14.7	–6.177	–1.364	87.0
49	CGCS 1449	103.339	5.693	5.90	127.304	40.678	77.0
50	CGCS 1457	103.487	9.353	6.80	–1.705	13.064	83.0
51	IT Mon	103.500	9.002	4.80	–5.971	–16.478	99.0
52	IRAS 06531-0216	103.918	–2.338	1.93	13.026	–5.064	39.4
53	IRAS 07073-1944	107.385	–19.827	5.31	–6.024	1.615	54.6
54	HX CMa *or* IRAS 07098-2012	108.017	–20.290	1.64	8.212	6.574	11.5
55	IRAS 07161-0111	109.662	–1.281	2.92	–13.050	–5.399	20.6

Table 1 *Continued.*

ID	Name	α (°)	δ (°)	d (kpc)	μ_ℓ^* (mas yr^{-1})	μ_b (mas yr^{-1})	V_r (km s^{-1})
56	[W71b]007–02	114.259	–19.549	4.16	–1.218	7.444	57.6
57	V471 Pup	115.275	–26.422	4.0	–1.088	3.147	90.5
58	IRAS 07546–2511	119.177	–25.996	6.26	–5.209	–4.908	96.5
59	[ABC89]Pup38	120.780	–26.575	11.79	1.377	3.122	60.2
60	FF Pup	120.898	–24.077	3.62	3.775	–8.49	48.3
61	V346 pup	122.704	–32.868	1.26	22.389	–36.487	–18.8
62	IRAS 08119–3627	123.450	–36.616	2.83	9.662	7.51	–5.30
63	[ABC]Ppx40	125.422	–34.957	4.92	–8.735	–2.951	64.8
64	V1568 Cyg *or* IRAS 21366+4529	324.633	45.713	2.54	1.234	1.982	30.2
65	IRAS 21383+4513	325.053	45.455	2.61	2.073	4.307	–21.5
66	V1732 Cyg	325.299	46.518	6.10	7.136	7.84	–93.0
67	V1428 Cyg	328.041	47.820	6.30	–8.818	3.414	–77.0
68	V1342 Cyg	329.340	49.900	4.30	–1.930	–0.526	–80.0
69	V1410 Cyg	329.610	49.643	4.00	–2.978	7.103	–66.0
70	PU Lac	332.273	50.466	5.70	4.417	0.165	–74.0
71	CGCS 5592	332.379	52.192	5.50	1.286	1.294	–36.0
72	LW Lac	332.536	51.666	4.20	–2.210	0.337	–82.0
73		342.144	54.939	4.60	–5.038	–7.869	–56.0
74	IRAS 23174+5941	349.923	59.972	4.58	–9.915	21.046	–55.0

The equatorial coordinates (α, δ) are given at the Epoch J2000.0 frame. The symbol d is the heliocentric distance of the star.

$V_0 = 220\,\mathrm{km\,s^{-1}}$ for the LSR motion (Kerr & Lynden-Bell 1986). R is the distance of the object to the Galactic center, derived from $R = \sqrt{R_0^2 + d^2\cos^2 b - 2R_0 d\cos b\cos\ell}$. According to the statistical analysis from the individual determination by Reid (1993), $R_0 = 8.0\pm0.5\,\mathrm{kpc}$ is currently considered as the best value. Because of the $\sin\ell$ term in the denominator, objects nearer than 30° from the anti-center ($\ell = 180°$), where V_{rot} is not well defined, are rejected. For stars outside the dashed lines (which indicate the directions $\ell = 150°$ and $\ell = 210°$) in Figure 1, the rotation curve is displayed in Figure 4. It outlines a virtually flat rotation which nearly equals the LSR rotation speed V_0. The slope does not significantly deviate from zero. However, due to the contribution of stars farther than $12\,\mathrm{kpc}$, the rotation curve shows a declining trend. Because the uncertainties in distance measurements are not given and the standard errors of radial velocities are not provided for all stars, we simply set 10% for the distance uncertainty similar to that adopted by Demers & Battinelli (2007) and $\pm15\,\mathrm{km\,s^{-1}}$ as the random part in radial velocities, which is the upper limit of the errors of radial velocities. See error bars in Figure 4.

3.2 Rotation Curve from Proper Motions and Radial Velocities

Based on the cross-identified parameters of C stars listed in Table 1, we can perform intensive analysis of the rotation curve of the outer disk without the circular motion assumption. In order to describe the motion, we adopt the conventional Galactic coordinate system (x, y, z) in the direction of the Galactic center, the Galactic rotation, and the north Galactic pole. Since the position (ℓ, b, d) and the space velocity relative to the Sun (μ_ℓ^*, μ_b, V_r) are known, the three components of velocity in the rectangular system are

$$\begin{aligned} V_x &= V_r\cos\ell\cos b - \kappa d\mu_\ell^*\sin\ell - \kappa d\mu_b\cos\ell\sin b,\\ V_y &= V_r\sin\ell\cos b + \kappa d\mu_\ell^*\cos\ell - \kappa d\mu_b\sin\ell\sin b,\\ V_z &= V_r\sin b + \kappa d\mu_b\cos b, \end{aligned} \tag{2}$$

where κ is a constant factor ($\kappa = 4.74047$).

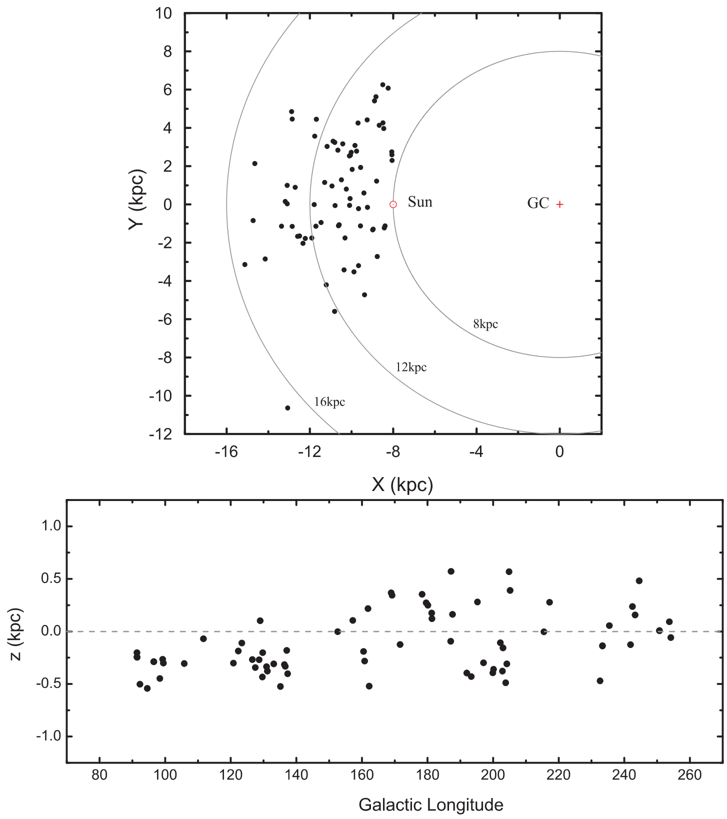

Fig. 3 Distribution of the stars in Table 1. The top panel shows the distribution onto the Galactic plane similar to Fig. 1. We should notice that the sample is a subset of Fig. 1. The bottom panel illustrates their vertical distribution versus Galactic longitude. The lack of objects near $z = 0$ is due to high absorption in the Galactic plane.

Considering the theme of the present paper, we will, practically, describe the problem on the Galactic plane. Supposing the Galactic center is at rest, the velocity vector $\boldsymbol{V}' = (V_x', V_y')$ on the xy plane relative to the Galactic center shall have the following form:

$$\begin{aligned} V_x' &= V_x + U_\odot, \\ V_y' &= V_y + V_\odot + V_0. \end{aligned} \tag{3}$$

The position vector $\boldsymbol{r}' = (x', y')$ pointing from the Galactic center to the C star can be expressed as follows:

$$\begin{aligned} x' &= d \cos \ell \cos b - R_0, \\ y' &= d \sin \ell \cos b. \end{aligned} \tag{4}$$

Projecting $\boldsymbol{V}'$ onto $\boldsymbol{r}'$, we obtain the rotation velocity

$$\boldsymbol{V}_{\rm rot} = \boldsymbol{V}' - (\boldsymbol{V}' \cdot \boldsymbol{r}')\, \frac{\boldsymbol{r}'}{|\boldsymbol{r}'|}, \tag{5}$$

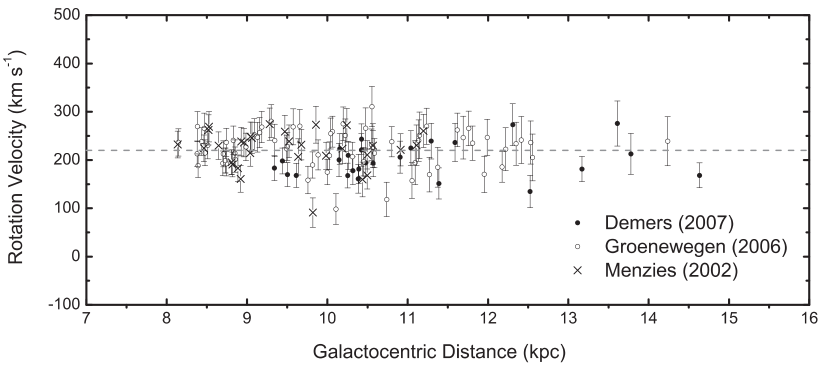

Fig. 4 Rotation curve of the outer disk as defined by carbon stars (outside of the dash-dotted lines in Fig. 1) derived from radial velocities only, with $R_0 = 8.0\,\mathrm{kpc}$ and $V_0 = 220\,\mathrm{km\,s^{-1}}$. The symbols are the same as those in Fig. 1. The dashed line is a constant rotation curve at $218\,\mathrm{km\,s^{-1}}$ for the whole sample.

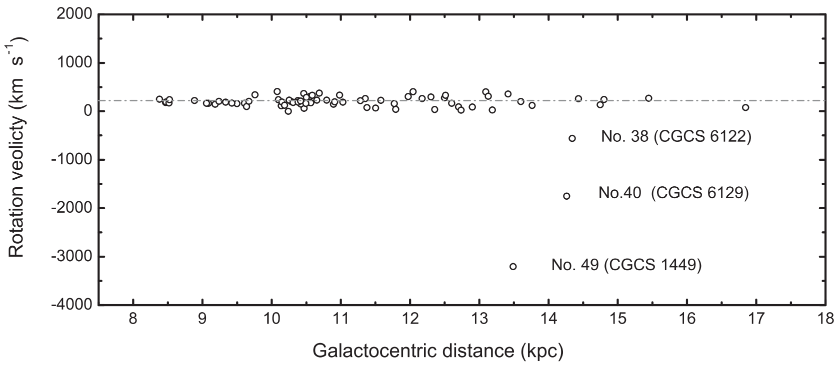

Fig. 5 Rotation curve of the outer disk as defined by carbon stars, with $R_0 = 8.0\,\mathrm{kpc}$ and $V_0 = 220\,\mathrm{km\,s^{-1}}$, as the dashed line indicates. The three marked objects with unusual large rotation velocities are CGCS 6122, CGCS 1449 and CGCS 6129.

which is the component of $\boldsymbol{V}'$ perpendicular to $\boldsymbol{r}'$. Figure 5 shows the resulting rotation curve derived from the combination of radial and tangential velocities of 74 C stars in Table 1. The three marked stars, which show extremely large velocities, are listed as No. 38 (CGCS 6122), No. 40 (CGCS 6129) and No. 49 (CGCS 1449). The example CGCS 1449, which is taken as an example, is located at $(208.1°, +3.0°, 5.9\,\mathrm{kpc})$ in the Galactic coordinate system and its velocity relative to the Sun is $(127.3\,\mathrm{mas\,yr^{-1}}, 40.7\,\mathrm{mas\,yr^{-1}}, 77\,\mathrm{km\,s^{-1}})$. The rotational velocity is dominated by the transverse component, which is actually larger than $3500\,\mathrm{km\,s^{-1}}$. It is noticed that the outlier C stars have unusually large proper motions for their distances and they should be removed according to the 3σ principle for further analysis. Figure 6 displays the results of the remaining data set. By fitting the data of the rotation velocities, we find a fairly flat rotation curve at $210 \pm 12\,\mathrm{km\,s^{-1}}$. The error bars are not plotted for concision of the picture. The farthest star in Figure 6 (No. 59 in Table 1) has a rotation velocity remarkably lower than V_0, which could suggest that the rotation curve of the Galaxy is decreasing. However, the lack of data points prevents us from drawing further conclusions.

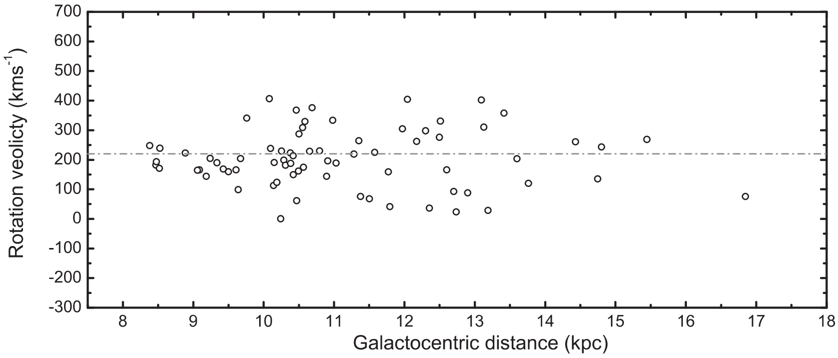

Fig. 6 Same as the previous figure, but the three outlier stars were rejected.

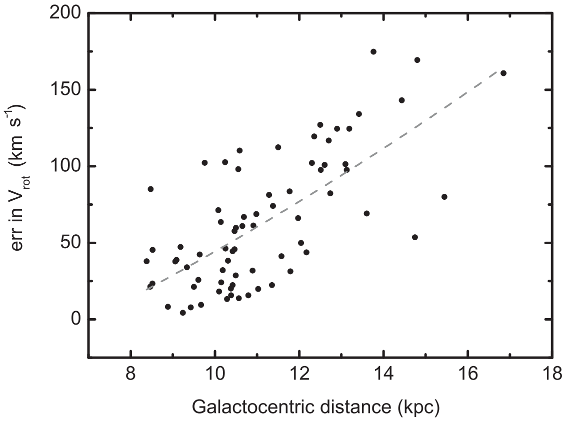

Fig. 7 Standard errors of rotation velocities. The error of $V_{\rm rot}$ takes into account 10% uncertainty in distance determination, a $\pm 15\,{\rm km\,s^{-1}}$ random part in radial velocities, proper-motion errors, and velocity dispersions for the carbon stars.

On a rotation curve plotted like in Figure 6, the effect of errors on distances will be enlarged, since the distance (d) enters the calculation of both R and $V_{\rm rot}$. Because of the dependence of tangential velocities on distances other than the radial velocities, the adoption of proper motions will lead to some more uncertainties and scatters for the results, compared to those obtained from radial velocities only. Taking into account the uncertainties of distances, proper-motion errors and the velocity dispersions for carbon stars, the standard errors of $V_{\rm rot}$ values are roughly hundreds of kilometers per second. Figure 7 depicts the tendency of uncertainties versus galactocentric distance. For a faint star at a large distance from the Sun, the proper motion uncertainty should be pronounced. As mentioned in the previous section, the typical values of $\sigma_{\mu_\ell^*}$ and σ_{μ_b} of selected C stars are 3–6 ${\rm mas\,yr^{-1}}$. The corresponding uncertainty in transverse velocity lies in the range from 100 to 200 ${\rm km\,s^{-1}}$ for a star located $5\,{\rm kpc}$ away from the Sun. On the other hand, the late-type C stars show markedly larger velocity dispersions than young disk stars. Blaauw & Schmidt (1965) suggest that the dispersions of carbon stars are: $\sqrt{\langle u^2\rangle} = 48$, $\sqrt{\langle v^2\rangle} = 23$ and $\sqrt{\langle w^2\rangle} = 16$ in ${\rm km\,s^{-1}}$. The second component $\sqrt{\langle u^2\rangle}$ in the direction of Galactic rotation is the major part that contributes to the error in rotation velocity.

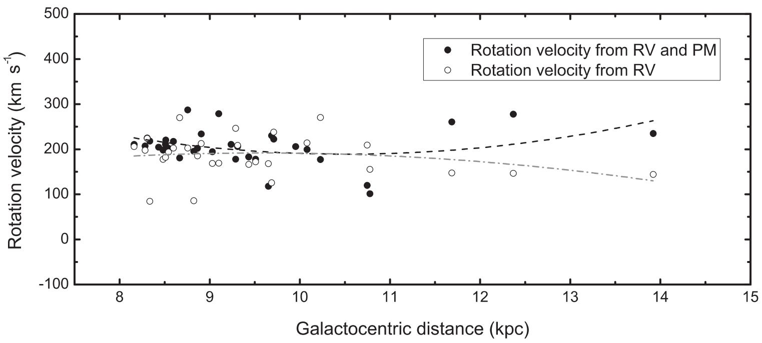

Fig. 8 Rotation velocities show divergence, especially at the end of the rotation curve. The open circles show the rotation velocities from radial velocities, and the filled circles the values after adding the transverse velocities. For the first method, data too close to the anti-center are not plotted.

4 DISCUSSION

The determination of the rotation curve presented in this paper combines radial velocities and proper motions of carbon stars, so it is more complicated to interpret than the method based on radial velocities alone.

To investigate the difference between the two methods, we tried to find a more homogeneous C star sample with three-dimensional velocities. Starting from the CGCS3, the first step in obtaining the cool carbon star sample near the Galactic disk is to match the star positions of CGCS3 with those in the "UCAC3C star candidate list." However, the range of latitude $|b| < 6°$ was replaced with $3° < |b| < 6°$ to avoid extremely low latitudes where the estimates of reddening are not quite reliable (Schlegel et al. 1998; The IPAC extinction Web calculator site is *http://www.ipac.caltech.edu/forms/calculator.html*). The matching criterion is a positional agreement to within 2 arcsec. This is equal to the poorest astrometric accuracy in the survey contributing to CGCS3. The radial velocities were obtained from the General Catalog of mean radial velocities (GCRV) (Barbier-Brosat & Figon 2000) and/or the second version of the catalog of radial velocities of Galactic stars with high precision astrometric data (CRVAD-2) (Kharchenko et al. 2007). In all, 40 C stars with full astrometric data were identified in which 7 common stars were recognized in Table 1 (see Table 2). Thus, the C stars from CGCS3 have their positions and proper motions in UCAC3 and radial velocities from GCRV or CRVAD-2. We would assume here that all selected objects are cool carbon stars.

The coordinates of each C star were put into the NED (NASA Extragalactic Database) extinction calculator (Schlegel et al. 1998) to get individual reddening and extinction in K magnitude (A_K). Nine sources were excluded due to the high extinction $E(B-V) > 1.2$. Then, intrinsic colors were fed into the following equation of absolute magnitude in the K-band reviewed by Demers & Battinelli (2007):

$$M_K = -6.31 - 0.99(J-K)_0, \tag{6}$$

with $(J-K)_0 = (J-K) - E(J-K)$. Assuming a distance modulus $\mu_{\rm LMC} = 18.5$ and a mean interstellar extinctions $E(B-V) = 0.13$ for LMC, the corresponding extinctions for the 2MASS photometries are $E(J-K) = 0.535E(B-V)$ (Mauron 2008). Mauron et al. (2004), in their study, compared the distance scales of the R-band and the K-band of C stars in the LMC and suggested that near-infrared based distance is more reliable than those from other estimation methods. The natural dispersions of the K-band absolute magnitudes of C stars are presumably no larger than $0.3\,\rm mag$ (Weinberg & Nikolaev 2001) corresponding to 25 percent in relative accuracy of distance.

Table 2 Carbon Stars from UCAC3 and CGCS3

ID	CGCS	GCRV/CRVAD-2	$\alpha(°)$	δ (°)	K	$E(B-V)$	A_K
1	2	181 / Null	1.435	65.516	7.236	1.336	0.490
2	43	587 / 930	5.612	59.193	3.286	0.744	0.273
3	54	816 / Null	6.301	68.032	5.070	1.170	0.430
4	55	823 / Null	6.326	88.286	6.164	1.810	0.664
5	114	1300 / Null	11.801	67.307	6.479	1.202	0.441
6	125	1040 / Null	13.101	47.415	5.422	1.119	0.411
7	136	Null / 2073	13.724	58.563	2.218	0.604	0.222
8	152	1626 / Null	15.023	67.623	5.783	1.170	0.429
9	155	1644 / Null	15.133	67.343	6.439	1.239	0.455
10	159	1654 / Null	15.232	67.345	4.725	1.236	0.454
11	190	2292 / Null	18.558	65.860	3.774	1.533	0.563
12	217	2494 / Null	20.913	65.938	5.889	1.337	0.491
13	248	2879 / Null	25.235	65.566	6.668	1.060	0.398
14	252	2930 / Null	25.645	66.037	6.277	1.468	0.530
15	384	4281 / 6092	39.679	55.767	4.263	0.600	0.220
16	581	6046 / Null	59.941	114.528	4.454	0.695	0.255
17	701	6750 / 9877	67.430	39.867	1.306	0.592	0.217
18	797	7323 / 10706	73.145	38.506	1.395	0.875	0.321
19	806	Null / 10776	73.563	49.900	2.928	0.887	0.322
20	836	7619 / 11138	75.846	50.633	1.440	0.708	0.260
21	841	7627 / Null	75.956	48.120	4.311	0.590	0.217
22	874	7808 / 11435	77.799	29.639	4.019	0.577	0.212
23	950	Null / 12194	82.334	43.409	3.970	0.561	0.206
24	990	8484 / 12425	83.606	24.853	3.256	0.959	0.352
25	1042	Null / 13020	86.414	20.695	0.355	0.779	0.286
26	1179	9915 / 14239	92.721	26.015	0.821	0.591	0.217
27	1222	10175 / 14605	94.425	8.520	1.856	0.472	0.173
28	1246	Null / 14815	95.492	7.349	2.322	0.492	0.181
29	1373	Null / 15771	100.802	–8.758	3.156	0.634	0.233
30	1489	11307 / 16364	104.590	6.167	1.811	0.261	0.096
31	1659	Null / 17239	110.030	–20.333	4.443	0.874	0.331
32	1695	Null / 17385	110.911	–22.970	3.045	1.554	0.570
33	1750	12168 / Null	112.934	–9.467	5.246	0.289	0.106
34	2024	Null / 19014	120.924	–23.836	4.148	0.260	0.095
35	2051	13079 / 19072	121.333	–38.777	2.762	1.095	0.402
36	2064	13111 / 19136	121.874	–22.913	2.065	0.264	0.097
37	2353	14176 / Null	132.654	–36.069	5.217	0.390	0.143
38	5494	33356 / 50479	328.807	50.497	1.952	0.629	0.231
39	5577	Null / 50913	331.666	48.452	2.722	0.341	0.125
40	5728	34594 / 52341	341.463	55.076	4.537	0.606	0.222

The second and third columns of the table indicate the running number in the CGCS3 and GCRV / CRVAD-2 respectively. “Null” means no matched star in the corresponding catalog. K, $E(B-V)$ and A_K are measured in mag.

The heliocentric distances are calculated using apparent magnitudes m_K, absolute magnitudes M_K and the extinction A_K. Rotation velocities are computed according to Equations (1) and (5). Figure 8 shows a comparison of the results from the two formulae. We can see from the picture that within a range less of than 3 kpc from the Sun, the rotation curves from the two methods are firmly consistent. The presence of distinction beyond $11\,\mathrm{kpc}$, where there are fewer data points, may be caused by the distance and proper-motion uncertainties for faint stars which will play a more important role as the distance increases. In the case of constant rotation, we find $\overline{V}_{\rm rv} = 186 \pm 5\mathrm{km\,s^{-1}}$ with $\sigma_{V_{\rm rv}} = 45\,\mathrm{km\,s^{-1}}$ and $\overline{V}_{\rm rv\&pm} = 206 \pm 15\mathrm{km\,s^{-1}}$ with $\sigma_{V_{\rm rv\&pm}} = 79\,\mathrm{km\,s^{-1}}$. The results show coherence on account of their errors. The other side is seen from the comparison that the rotation curve from radial velocities is definitely correct, because no obvious deviation is found between the two methods in the sense of statistics.

5 CONCLUSIONS

On the basis of radial velocities, proper motions, and heliocentric distances of cool carbon stars near the Galactic plane toward the anti-center direction, we have re-investigated the rotation curve of the outer disk without the circular motion assumption. The carbon stars defined a flat rotation curve between $R = 8\,\mathrm{kpc}$ and $R = 15\,\mathrm{kpc}$, which has a mean rotation velocity $V_{\mathrm{rot}} = 210\,\mathrm{km\,s^{-1}}$, with an internal error of about $12\,\mathrm{km\,s^{-1}}$. This value of constant rotation velocity is firmly consistent with previous studies. For the method using three dimensional parameters, the standard deviation of the results is markedly larger than the traditional one. The mismatch can be attributed to the uncertainties of distances and proper-motion errors for faint stars which play a more important role in our process of calculation. We find no deviation between the two methods. As a byproduct, a C star list with precision positions and velocities is recognized via cross-identification.

Acknowledgements This work was funded by the National Natural Science Foundation of China (NSFC) (Grant Nos. 10673005 and 10973009). This research makes use of data products from UCAC3 (U.S. Naval Observatory) and we are indebted to Dr. N. Zacharias who sent us the DVD disk containing their up-to-date research achievements. This work has also made use of the SIMBAD database operated at CDS, Strasbourg, France.

References

Alksins, A., Balkavs, A., Dzervitis, U., Eglitis, I., Paupers, O., & Pundure, I. 2001, Bal. Astron., 10, 1 (CGCS3)
Aumer, M., & Binney, J. J. 2009, MNRAS, 397, 1286
Barbier-Brossat, M., & Figon, P. 2000, A&AS, 142, 217 (GCRV)
Battinelli, P., & Demers, S. 2005, A&A, 442, 159
Battinelli, P., Demers, S., & Mannucci, F. 2007, A&A, 474, 35
Blaauw, A., & Schmidt, M. 1965, Galactic Structure (Chicago: Univ. of Chicago Press)
Blanco, V. M. 1965, in Stars and Stellar System, Galactic structure, eds. A.Blaauw, & M. Schmidt (Chicago: Univ. of Chicago Press), 5, 241
Blitz, L., & Spergel, D. N. 1991, ApJ, 370, 205
Cioni, M.-R. L., & Habing, H. J. 2003, A&A, 402, 133
Davidge, T. J. 2005, AJ, 130, 2087
Demers, S., & Battinelli, P. 2007, A&A, 473, 143
Fich, M., Blitz, L., & Stark, A. A. 1989, ApJ, 342, 272
Groenewegen, M. A. T., Sevenster, M., Spoon, H. W. W., & Pérez, I. 2002, A&A, 390, 511
Kang, A., Sohn, Y.-J., Kim, H.-L., Rhee, J., Kim, J.-W., et al. 2006, A&A, 454, 717
Kerr, F. J., & Lynden-Bell, D. 1986, MNRAS, 221,1023
Kharchenko, N. V., Scholz, R.-D., Piskunov, A. E., et al. 2007, Astron. Nachr., 328, 889 (CRVAD-2)
Mauron, N., Azzopardi, M., Gigoyan, K., & Kendall, T. R. 2004, A&A, 418, 77
Mauron, N. 2008, A&A, 482, 151
Menzies, J. W., Feast, M. W., & Whitelock, P. A. 2006, MNRAS, 369, 783
Nikolaev, S., & Weinberg, M. D. 2000, ApJ, 542, 804
Pont, F., Mayor, M., & Burki, G. 1994, A&A, 285, 415
Pont, F., Queloz, D., Bratschi, P., & Mayor, M. 1997, A&A, 318, 416
Reid, M. J. 1993, ARA&A, 31, 345
Schlegel, D. J., Finkbeiner, D. P., & Davis, M. 1998, ApJ, 500, 525
Weinberg, M. D., & Nikolaev, S. 2001, ApJ, 548, 712
Westerlund, B. E. 1965, MNRAS, 130, 45
Zacharias, N., Urban, S. E., Zacharias, M. I., Wycoff, G. L., Hall, D. M., et al. 2004, AJ, 127, 3043
Zacharias, N., Finch, C., Girard, T., Hambly, N., Wycoff, G., et al. 2010, AJ, 139, 2184 (UCAC3)